

Seismic behaviour of earth reinforcement walls

R.A. Sofronie

UNESCO Chair Ecoland, University of Bucharest, Romania

C.A. Taylor

Earthquake Engineering Research Centre, University of Bristol, UK

F. Iosif

Technical University of Civil Engineering, Bucharest, Romania

ABSTRACT: The paper presents the experimental results of a test programme performed on the shaking table of Bristol University, UK. Two similar models of reinforced soil retaining walls, one of conventional type and another self-confined, have been investigated. Both models supported the same elastic structure and were submitted to inputs of increasing intensities. The seismic behaviour of the models was comparatively analysed with the aid of cumulative diagrams of settlements, horizontal displacements and response accelerations. The ultimate limit state occurred by tilting of the facing, but the two models reached this state differently. The numerical models revealed the local phenomena that developed in the reinforced soil as well as the large influence of the elastic structure. Both conceptual design and the development of numerical analysis are supported by the results.

1 INTRODUCTION

Eurocode 8 does not contain provisions for seismic design of earth reinforcement. Reinforced soil structures for retaining walls, abutments and slopes are currently designed according to BS 8006-95 and DIN 4017. There are two criteria of design: 1) external stability; 2) internal stability. Confining earth reinforcement improves the stability of both types (Sofronie & Feodorov 1995, 1998).

The buildings supported by soil structures are currently considered only as static surcharges. There are no provisions for soil-structure interaction under seismic actions. The former tests carried out on two pairs of models, for conventional and confined retaining walls, one in Bristol, UK in 1998 and another to Iasi, Romania in 1999, offered some information of practical interest (Sofronie, Taylor & Greening 2000). Indeed, earth reinforcement structures tend to settle continuously without collapse. Obviously, this stable behaviour is mainly due to the granular structure of the soil but also to its degree of compactness. Similarly, horizontal displacements occur as a consequence of facing tilt. The response accelerations characterise the dynamic behaviour of earth reinforcement and emphasise the amplification or attenuation phenomena developing in models during earthquakes.

Now the problem was to investigate the influence of elastic structures on earth reinforcement retaining walls. By conducting the testing program according to the same principles used for the former program and comparing the results one could assess the influencing factors. However, the current research was

more advanced. First the facings were fixed with hinges at their bottom and in this way only a single DOF was allowed, that of tilting. Secondly the steel cables were anchored in the backfill allowing in this way a self-confining mechanism of the model. Finally a numerical distinct element model based on the UDEC 3.10 program was developed.

The significance of the research is to assess the behaviour of the two types of reinforced earth structures in seismic conditions, to determine some practical recommendations for safe seismic design and to draw out some structural measures for mitigation of their seismic vulnerability.

2 MODEL SET-UP

For the two models, an existing shear stack was used. This is a flexible parallelepiped box, composed of aluminium rings alternately connected with rubber elements, specially designed to reproduce the field boundary conditions experienced by soil structures during earthquakes. The philosophy of modelling was to compare three phenomena developed under seismic actions, namely settlements, horizontal displacements and response accelerations, for the two types of retaining walls. Leighton Buzzard Sand was used for both infill and backfill. This is a siliceous, uniform and cohesionless sand with a unit weight (as placed) of 15.4 kN/m^3 and the internal friction angle $\phi' = 45^\circ$. As reinforcement Tensar geogrid SR55, with quality control strength of 55 kN/m and specific weight of 0.5 kg/m^2 , was adopted. The grids were fixed to the facing by nails at five

levels equally spaced at 150 mm. For the conventional wall they were carefully cut at $L=540$ mm, corresponding to the required aspect ratio $L/H=0.6$ (Fig. 1).

The self-confined wall was derived from the first model by shortening the grids to $L=360$ mm for an aspect ratio $L/H = 0.4$ and by adding the two steel cables of $\Phi = 6$ mm anchored in backfill. The idea of self-confinement is not new, it has been already tested on the shaking table of INCERC Iasi in 1999, but the results were not reported yet (Fig. 2).

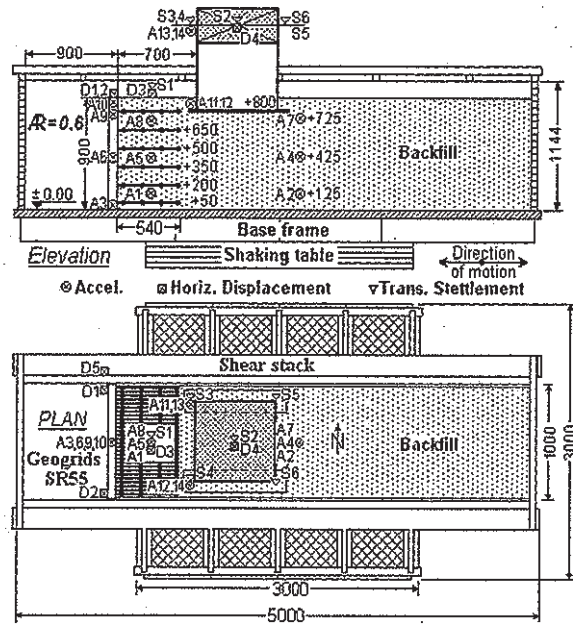


Figure 1. Model of the conventional walls.

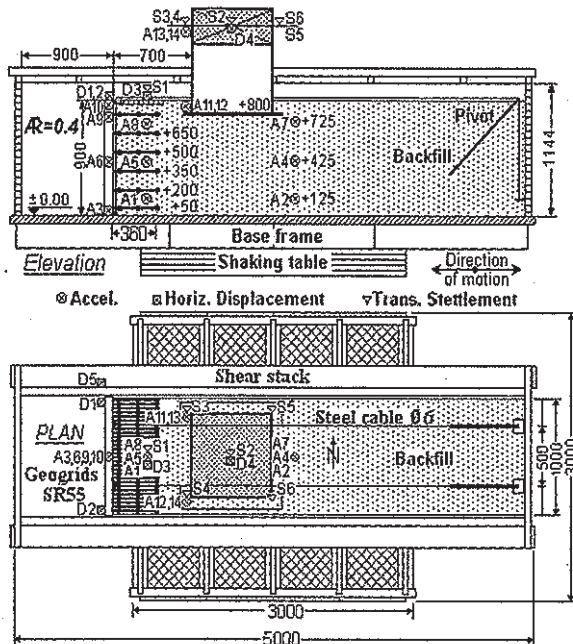


Figure 2. Model of the self-confined walls.

The innovation of this test was the elastic structure with one DOF. It was installed on the backfill in the most disadvantageous position for reinforced soil. Four loading cases were considered for the structure, with natural frequencies of 11 Hz, 6.1 Hz, 4.7 Hz and 3.4 Hz, respectively. Since this range of frequencies is much lower than the natural frequency of the earth reinforcement model of 30 Hz, there was no danger of resonance occurring in the oscillating system (Sofronie, Taylor & Crewe 2000).

3 RECORDING DEVICES

Twenty-eight channels of instrumentation monitored the actual motion of the shaking table and the behaviour of the model incorporated in the shear stack. Of these, 14 devices were used for the model itself, 10 for the elastic structure, 3 for the shaking table and 1 for the shear stack. The infill settlements and horizontal displacements were recorded with non-contacting transducers. Two wire-potentiometer transducers recorded the facing displacements. Response accelerations were recorded at six positions in the soil and at four positions on the facing. The settlements of the elastic structure were measured at the four corners and at the centre of the roof mass. Orthogonal horizontal response accelerations of the structure were measured at the foundation and roof. The shaking table accelerations were measured in the three principal directions. The horizontal displacement of the shear stack was monitored at one location. For the accelerations induced in the sand, 6 unidirectional piezoelectric accelerometers were placed at different levels: 3 in the infill between the geogrid reinforcements, and 3 in the backfill (Figs. 1 and 2). These miniature accelerometers, with 0.7 mm in diameter and 4.5 g in weight, were used so as to reduce the disturbance to the material behaviour. They were mounted inside small, light perspex boxes size so that the whole unit had the same mass density of the sand, and were positioned during sand deposition. A thin layer of sand was glued to each side of the boxes to guarantee good contact with the adjacent granular material. All accelerometers were connected by thin flexible coaxial cables. The cables were protected during the experimental tests to prevent potential damage induced by the sand movements. Before starting the testing program, all recording devices were carefully calibrated. In addition, the initial level of sand was manually mapped in 13 vertical cross sections. After the collapse of each model, the final surfaces were mapped again. By difference of measured heights the controlling values of settlements in both models were been obtained. Indeed, these values have been compared with the recorded values for settlements and a good agreement was found. The aspect ratio of area affected by collapse was $L/H=2.45 - 2.80$.

4 TESTING PROGRAM

The six degrees of freedom shaking table at Bristol University was opened in 1987. It has a cast aluminium platform measuring 3 m by 3 m, weighing 30 kN, and has a maximum payload of 150 kN. The platform is driven by eight 50 kN servo-hydraulic actuators, four acting horizontally around the perimeter and four acting vertically at the corners. The platform has peak displacements of ± 150 mm in all translation axes, peak velocities of 0.5 m/s and peak bare platform accelerations of 4.8g horizontally and over 7.5g vertically. A PC-based real-time digital control system allows a wide range of recorded and synthetic earthquake and other motions to be reproduced by the shaking table. Up to 64 data acquisition channels are available (Taylor 1997).

For fulfilling the three objectives of the comparative test programme, a single degree of freedom shake was applied in the longitudinal direction of the models. Three types of input excitations were successively induced: the El Centro'40 acceleration (Fig. 3), a Eurocode 8 compatible artificial acceleration (Fig. 4) and a sine dwell function with a frequency of 5 Hz (Fig. 5). Since the dominant input frequencies were much lower than model natural frequency of 30 Hz, there was no danger of resonance occurring in the soil deposit at low levels of table acceleration.

All inputs were alternately induced with gradually increasing intensities beginning with 0.1g up to over 1g. For each of four weights of the elastic structure, namely 50 kg, 100 kg, 150 kg and 250 kg, the three types of inputs were successively induced. The first model of a conventional wall was shaken with

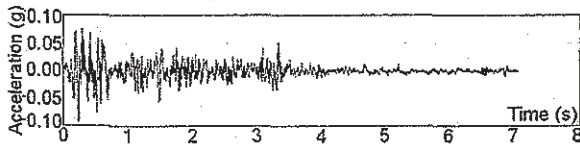


Figure 3. El Centro'40 acceleration time history.

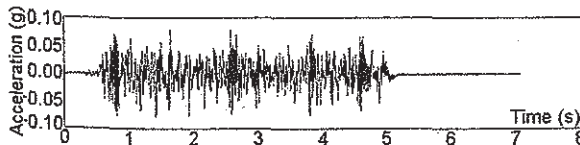


Figure 4. Eurocode 8 acceleration time history.



Figure 5. Sine dwell acceleration time history.

52 quakes, and the second one with 57. The El Centro'40 input, as the weakest of the three inputs, was induced 13 times in each model. The Eurocode 8 input was induced 19 times in the model of conventional walls and 22 times in the model of self-confined walls. The sine dwell quasi-harmonic function has a constant length with increasing amplitude from zero to the maximum value over the first ten cycles, constant amplitude over the subsequent twenty cycles, with the amplitude decreasing down to zero over the last ten cycles. This kind of input motion is more severe than the former two but it allows clear investigation of the kinematics of soil structure models and their behaviour at acceleration values close to the ultimate limit state. It was induced with gradually increasing intensities 20 times in the model of conventional walls and 22 times in the model of self-confined walls.

At the end of the test program, strong sine dwell inputs were induced in each model. The conventional wall model yielded at 1.25g by facing tilt, while the self-confining wall failed similarly, but at 1.69g and only after one of the two steel anchorage pulled out. Both cases of collapse were strongly influenced by the elastic structure under its maximum loading (Figs. 6&7). From the 109 tests performed 3,052 recordings in real time were obtained.

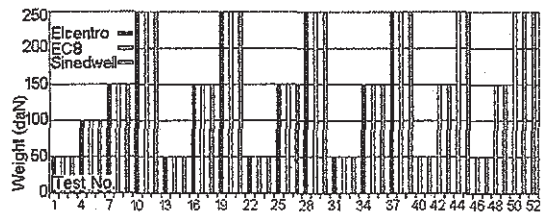


Figure 6. Testing program for conventional wall model.

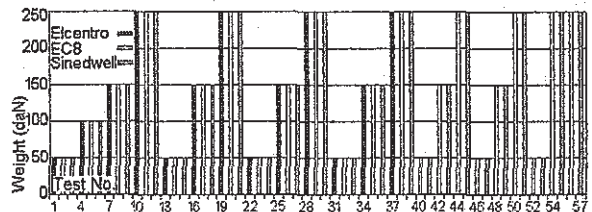


Figure 7. Testing program for self-confining wall model.

5 SETTLEMENTS

The settlements of the two models were recorded at the top of the infill (S1 at the level +900 mm) and at the top of the elastic structure (S2 at the level of +1,220 mm), both located on the longitudinal axis of symmetry. They were measured from one test to the subsequent one in a cumulative manner. For each model the specific behaviour was observed of the in-

fill and backfill under the three types of inputs with increasing intensities, and then the settlements of the two models were compared. In the case of the conventional wall, no significant settlements were recorded during the first succession of 23 quakes. After the sine dwell quake, no.24, with an intensity of 0.3g, the infill settled by 8 mm and the backfill by 4.4 mm. During the next quakes the settlements gradually progressed. Some larger values occurred after quake no. 47 but they were not critical. Collapse occurred during quake no.52, under a sine dwell input of 1.25g, when the settlements reached 58 mm in the infill and 48 mm in the backfill. Then the facing tilt and the elastic structure inclined without overturning. It was a controlled yielding, similar to a *fail-safe* condition (Fig.8).

The self-confining wall behaved slightly different in settling. From the first quakes the anchoring cables relaxed little by little and the infill started to settle so that after quake no. 7 a cumulative value of 7 mm was recorded. The whole irregular shape of infill settlement diagram reflects the influence of both, on one side of the facing and on the other side of the elastic structure. At the same time the backfill continuously and uniformly settled. The collapse occurred during quake no. 57, also under a sine dwell, but at 1.69g and only after one of the two anchoring cables was pulled out. By coincidence the settlements reached 59 mm in the infill and 48 mm in backfill. The mechanism of yielding was similar, and during the collapse the synthetic reinforcement was not damaged (Fig.9).

By reporting the settlements to the increasing values of induced accelerations it appears that in both infill and backfill the main phenomena occurred when the intensities assumed values between 0.3g and 0.7g (Figs.10&11). The only difference between conventional and self-confining walls was that the later resisted longer and to intensities 35% higher.

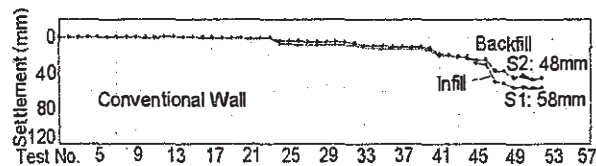


Figure 8. Settlements in the model of conventional walls.

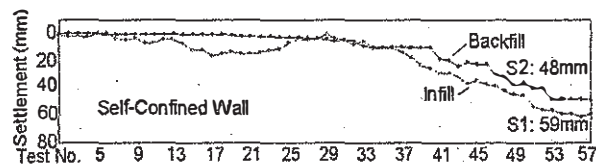


Figure 9. Settlements in the model of self-confined walls.

The shapes of the sand surface for both models before and after collapse were drawn from manual measurements. It is evident that due to anchoring steel cables the self-confined wall behaved much better and therefore was safer (Figs. 12&13).

6 HORIZONTAL DISPLACEMENTS

All measured displacements were in the downstream direction of the models and were influenced by both facing tilt and the elastic structure. In the case of conventional wall model the infill displaced more than the backfill and the influence of the elastic structure was not felt before quake no. 40. The last displacements before collapse were of 77 mm in the infill and 68 mm in backfill (Fig. 14). In the self-confining wall, the infill and backfill remained close

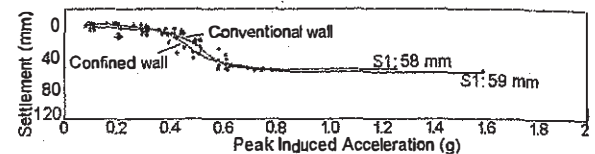


Figure 10. Infill settlements in the two tested models.

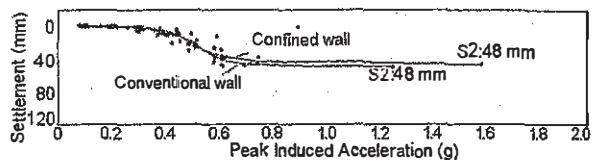


Figure 11. Backfill settlements in the two tested models.

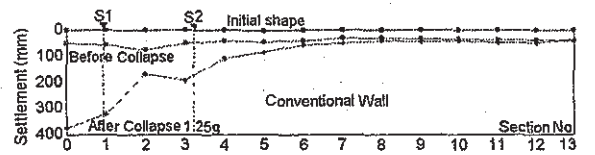


Figure 12. Conventional wall model before and after collapse.

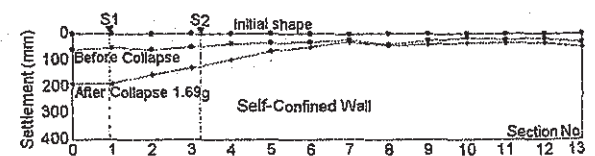


Figure 13. Self-confined wall model before and after collapse.

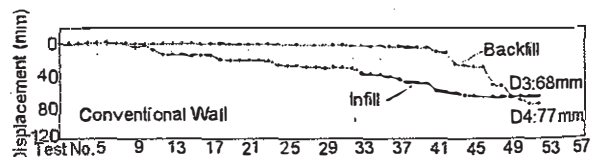


Figure 14. Displacements in conventional wall model.

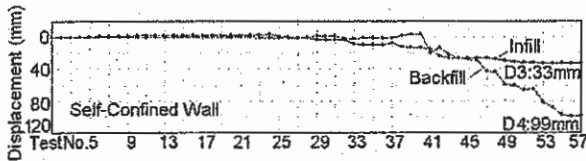


Figure 15. Displacements in self-confined wall model.

and behaved similarly during 46 quakes. Only after the anchoring cables started to yield (by pulling out of the anchorage) did the infill displacements increase and finally reach 99 mm, while in backfill the last recorded displacement was of 33 mm (Fig. 15).

By plotting the settlements with respect to the increasing values of induced accelerations, it appears that the infill of the conventional wall started to displace from the first quakes, while that of the self-confined wall only started after the input intensity reached about 0.4g. However, for intensities higher than 0.6g the infills in both models no longer displaced (Fig.16).

The backfill displaced similarly in both models for inputs under 0.4g. Further, for intensities between 0.5g and 0.6g, the backfill of the conventional wall model displaced by 77 mm and remained at this value until the collapse occurred at 1.25g. In the other model, the same phenomenon occurred, but in a larger range of intensities, namely between 0.4g and 0.8g, what indicates a better behaviour (Fig. 17).

Horizontal displacements were little influenced by the elastic structure; they mainly depended on the facing tilt. As concerns the self-confining procedure, it barely prevented the horizontal displacements, because the anchors were also moving together with the backfill. Only in the case of confining with a fixed cable were the horizontal displacements restrained.

The elastic structure was designed and constructed of steel members with only one horizontal DOF. Two of the structure's natural frequencies, 4.7 Hz and 6.1 Hz obtained for different loading cases, were rather near to the sine dwell excitation and therefore amplification phenomena could arise.

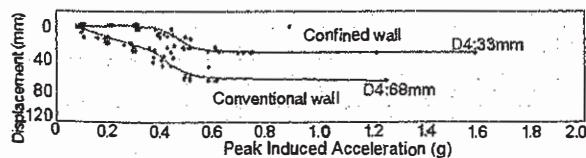


Figure 16. Infill displacements in the two tested models.

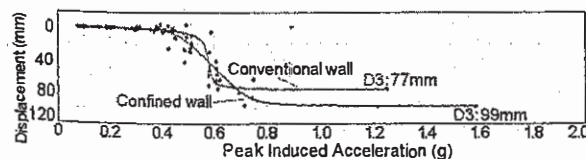


Figure 17. Backfill displacements in the two tested models.

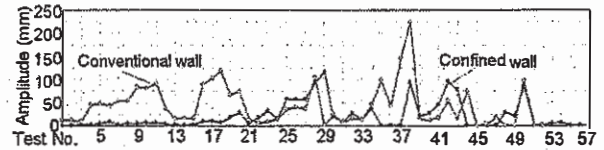


Figure 18. Dynamic response of the elastic structure.

However, the excitation time being too short, significant resonance did not occur. A selection of maximum amplitudes developed during each quake for both models are comparatively presented in two diagrams (Fig. 18). Surprisingly, the dynamic response of elastic structure located on the conventional wall was much stronger than in the case of the self-confined wall. A rigorous explanation of this behaviour could be given only after a mathematical analysis of the dynamic phenomena.

7 RESPONSE ACCELERATIONS

The dynamic behaviour of the elastic structure located on the two models was characterised with the aid of response accelerations recorded at its base and top. For practical reasons the ratio between peak the response acceleration (PRA) and peak induced acceleration (PIA) was considered. Values of this ratio larger than one show amplification, and those lower than one show attenuation.

The recordings obtained for both models show that at the base of the elastic structure the PRA/PIA ratio remained almost constant and assumed unit values. On the contrary, at the top-level, large amplifications occurred. The amplification ratio reached about 6.5 for the conventional wall model and 5.5 for the self-confining wall model (Figs.19&20). Again this different dynamic behaviour should be explained by mathematical analysis. It could be of practical interest when mitigation of seismic risk is considered.

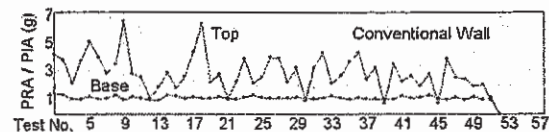


Figure 19. Dynamic behaviour of the elastic structure on conventional wall model.

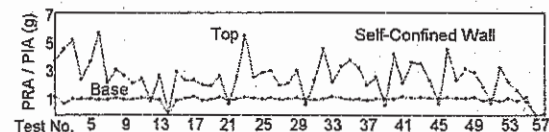


Figure 20. Dynamic behaviour of the elastic structure on self-confining wall model.

8 NUMERICAL ANALYSIS

With the aid of the UDEC 3.10 distinct element program, the two types of retaining wall were also numerically modelled and submitted to the same actions as the physical models tested on the shaking table (Fig. 21). The elastic structure was also modelled. However, the first results of the analysis brought more questions than answers. Under the seismic action at the bottom of soil structure a strong perturbation occurred. Since the direction of displacement vectors was nearly parallel with the reinforcement a special check would be necessary for that zone (Fig. 22). The upper layers of soil seemed to uplift and nothing prevented them from doing so. This would justify the need of confining soil structures and inducing over those layers some pressure.

As concerns the settlements, the analysis showed that the layers of reinforced soil detached and settled separately, mainly after the critical time occurred around second 4 (Fig. 23). This separation of layers is a strong reason for confining the reinforced soil. The same separation of layers also appeared when

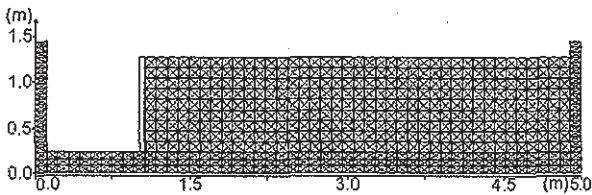


Figure 21. The shear stack with conventional retaining wall.

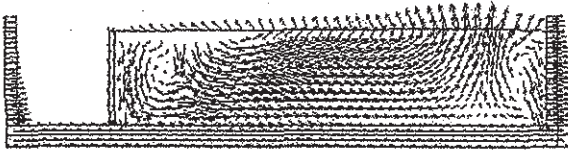


Figure 22. Displacement vectors for an input EC8 of 0.1g.

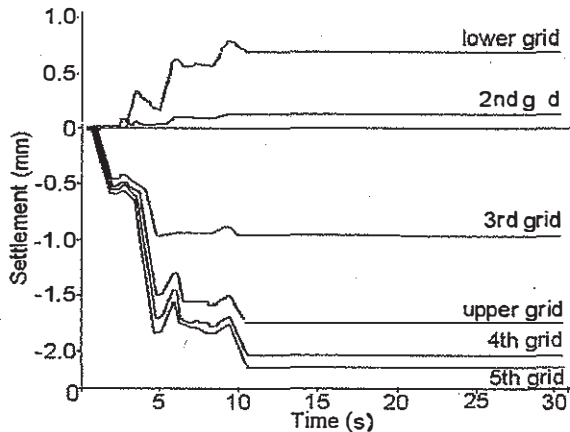


Figure 23. Infill settlements in conventional wall for 0.1g EIC.

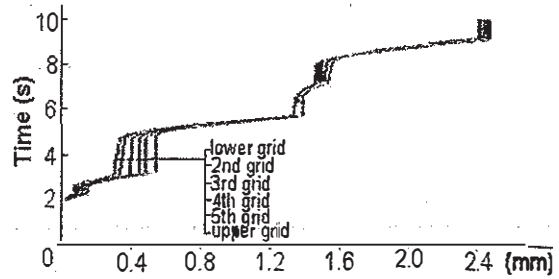


Figure 24. Horizontal displacements of facing for 0.1g EIC.

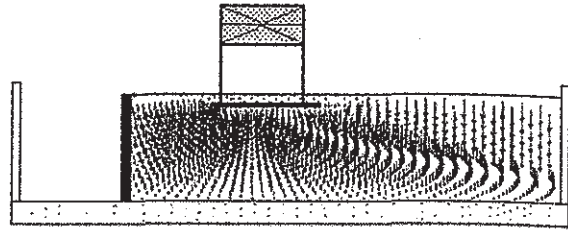


Figure 25. Displacement vectors in conventional wall model.

horizontal displacements were analysed (Fig.24). This problem could be of great concern for the behaviour of soil structures in seismic areas. Finally, the dynamic influence of the elastic structure was much larger than expected, and the reinforced zone was mainly affected (Fig. 25).

9 CONCLUSIONS

1. The three parameters: settlements, horizontal displacements and response accelerations satisfactorily characterise the seismic behaviour of earth reinforcement walls.
2. The comparative method adopted in both physical and numerical analyses proved useful by preserving only the common phenomena and allowing their critical review.
3. Even if the confining is still a theoretical concept any efforts to make it true are worthwhile because it brings safety and economies.

10 ACKNOWLEDGEMENTS

The financial support of the European Commission DGXII for Science, Research & Development through the Project INCO Copernicus IC15-CT96-0203 EUROQUAKE and ECOLEADER programme is gratefully acknowledged. Thanks are also due to the Company *Tensar International*, based in UK, for supplying the polymer grids used in testing programs.

REFERENCES

- Sofronie, R., Feodorov, V., 1995. Stability of Reinforced Slopes. *Proceedings of the 10th Danube-European Conference on Soil Mechanics and Foundation Engineering*. 12-15 September 1995 Mamaia, Romania, Vol.2, pp.423-428.
- Sofronie, R., Feodorov, V., 1998. Confining degree of Reinforced Soil Structures. *Proceedings of the 11th Danube-European Conference on Soil Mechanics and Foundation Engineering*, 25-29 May 1998, Porec, Croatia, pp.279-282.
- Sofronie, R. A., C. A. Taylor, & P. G. Greening 2000. Seismic resistant retaining walls of reinforced soil. *Proceedings of the 12th World Conf. on EQ Eng.* Auckland, N.Z., 30 Jan.-4 Feb. 2000, paper #2029.
- Sofronie, R.A., C. A. Taylor, & A. J. Crewe 2000 Mitigation of seismic risk by confining soil structures. *Proceedings of the Workshop on Mitigation of Seismic Risk – Support to Recently Affected European Countries*. Hotel Villa Carlotta, Belgirate (VB), Italy 27-28 November 2000, paper #44.
- Taylor, C. A., 1997: Large scale shaking tests of geotechnical structures. ECOEST/PREC8, Report No. 3.